
Effect of gold nanoparticles contrast agent concentration on X-ray diagnoses: Experimental and computational study

Mohamed I. Badawi¹, Moustafa M. Ahmed², Soheir M. I. El-kholy³, Nivan M. Fikry⁴,
M. S. Nasr Eldin⁵

¹Electrical Engineering Department, Alexandria University

²Prof. of Medical Biophysics, Medical Research Institute, Alexandria University and Vice Dean Faculty of Allied Medical Science, Pharos University in Alexandria

³Prof. & head of medical Biophysics Department Medical Research Institute, Alexandria University

⁴Prof. of Biophysics in Medical Research Institute, Alexandria University

⁵Assistant Lecturer in Radiology Department - Faculty of Applied Medical Sciences October 6 University

Email address:

mbadway007@yahoo.com (M. I. Badawi), moustafa.mohamed@pua.edu.eg (M. M. Ahmed),

sohairelkholy@yahoo.com (S. M. I. El-kholy), nivanfikry@yahoo.com (N. M. Fikry), mohamed_mri@yahoo.com (M. S. N. Eldin)

To cite this article:

Mohamed I. Badawi, Moustafa M. Ahmed, Soheir M. I. El-kholy, Nivan M. Fikry, M. S. Nasr Eldin. Effect of Gold Nanoparticles Contrast Agent Concentration on X-Ray Diagnoses: Experimental and Computational Study. *American Journal of Nanoscience and Nanotechnology*. Vol. 2, No. 4, 2014, pp. 63-69. doi: 10.11648/j.nano.20140204.11

Abstract: Nanotechnology applied to biological problems represents an emerging field with its potential to offer extremely sensitive diagnostics and targeted cancer therapies. Gold nanoparticles (GNPs) are of interest as potential in vivo diagnostic and as X-ray contrast agents, the electromagnetic coupling between three-dimensional gold nanoparticles (AuNPs) is investigated in different concentration. We report on the observation of multiplex electric field distribution between adjacent gold nanoparticles in the gap distance of AuNPs and on its edges. In this computational and exponential study we examine image reconstruction of electric field distribution occurs due to striking of x-ray on a gold nanoparticles at different concentration, also study the relation between gap distance between neighboring AuNPs. A CST STUDIO program used to calculate the electric field distribution. Electric field images of the gold nanoparticles as contrast agent demonstrate the potential of the approach for detecting the potential of gold nanoparticles in enhancing the image quality.

Keywords: X-Ray Cancer Diagnoses, Gold Nanoparticles, Imaging, Nanotechnology

1. Introduction

Colloidal gold (Au) was discovered by scientists as early as in the 4th century B.C. Since then, colloidal Au solutions have been employed particularly for medical purposes. The first intravenous injection of Au solution was performed in 1880 to treat alcoholism [1], on other hand one of the advantageous physical properties of Au is its high X-ray absorption when employed in X-ray imaging. Since its discovery by Röntgen in 1896 [2], X-ray imaging has expanded its unique territory in biomedical applications as one of the popular tools to see through a body nondestructively. X-rays have been developed for targeted researches and medical uses depending on the type of the

light or wave sources and generated energy regions. In this point, AuNPs-based X-ray imaging can provide a great potential in imaging technologies.

2. Colloidal Gold

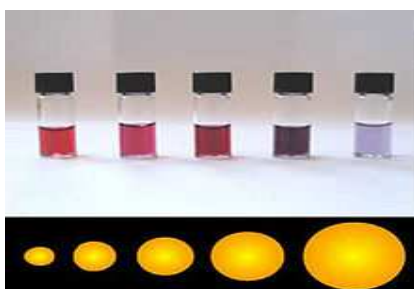
First Colloidal gold is a suspension (or colloid) of nanometer-size particles of gold in a fluid, usually water. The liquid is usually either an intense red color (for particles less than 100 nm) or blue/purple (for larger particles) [3]. Due to the unique optical, electronic, and molecular-recognition properties of gold nanoparticles, they are the subject of substantial research, with applications in a wide variety of areas, including electron microscopy, electronics, nanotechnology, and materials science. The

generation of colloidal gold nanoparticles was first described by Michael Faraday in 1857 when he described the synthesis of multicolored solutions (Fig. 1) by reacting gold chloride with sodium citrate [4]. Unbeknownst to him, what he actually described was the synthesis of colloidal gold nanoparticles that ranged from 12–47 nm in diameter. Since that time, gold nanoparticles have been used to meet a variety of needs in science and medicine.

In cancer research, colloidal gold can be used to target tumors and provide imaging and detection; these gold nanoparticles are surrounded with Raman reporters, which provide light emission that is over 200 times brighter than quantum dots, gold nanoparticles accumulate in tumors, due to the leakiness of tumor vasculature, and can be used as contrast agents for enhanced imaging [3].



(a)



(b)

Figure 1. Colloidal gold nanoparticles, the size difference causes the difference in colors.

3. Electric Field Around and between Nanoparticles

Metal nanoparticles have fascinating optical properties that differ greatly from the ones of their bulk counterparts. Metal nanoparticles absorb light at specific wavelengths due to the (localized) surface Plasmon resonance (SPR). The SPR has a high optical selectivity and thus metal nanoparticles can be used for applications in various fields from biomedicine to energy technology [5,7,8].

The SPR depends highly on the properties of the nanoparticles and the medium where the nanoparticles are embedded. The shape, size and material of the nanoparticles and the refractive index of the medium affect the intensity and position of the SPR. Various shapes, such as spheres, spheroids and shells, and sizes of metal nanoparticles have been studied to adjust the SPR into the desired wavelength

region without a considerable decrease in the intensity. Moreover, different nanoparticle concentrations and media have been used to adjust the SPR as well [5, 7, 8].

The incidence light or wave causes the electrons of the nanoparticle to delocalize forming an electric field opposite to the one of the wave. At specific frequencies, the electron oscillation is in resonance with the light wave. This phenomena is known as the (localized) surface plasmon resonance (SPR) (Fig. 2,3).

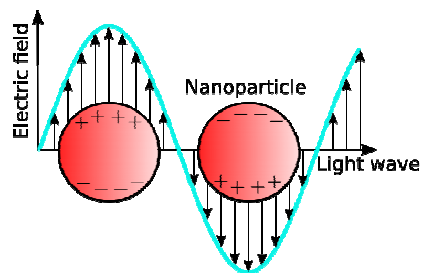


Figure 2. Nanoparticle (localized) surface Plasmon resonance (SPR).

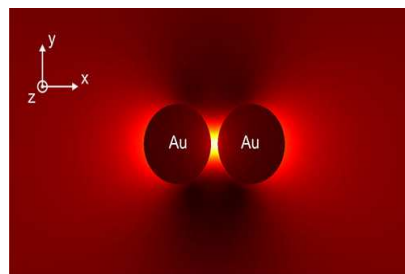


Figure 3. Electric field between two adjacent AuNPs.

4. Materials and Methods

4.1. The Phantom

The phantom used in this study made up of a Pyrex material, with 5 cylindrical holes with diameter 1 cm and 1 cm height, each of these cylindrical holes had been filled with a different concentrations of Colloidal gold nanoparticle (0.1ml,0.05ml,0.025ml,0.0125ml and 0.00625ml) (Fig.4.a,b).



(a)



(b)

Figure 4. Phantom 1. (a) Colloidal gold with concentrations (0.1, 0.05, 0.025, 0.0125 and 0.00325 ml/gm) (b) five Pyrex tubes of a 1 cm diameter and 1 cm height filled with Colloidal gold.

4.2. Pre Filling and Filling of Nanoparticles Protocol

- 1- Preparation of the contrast agent (Colloidal gold).
- 2- Preparation of the phantom.
- 3- Fill the phantom with the contrast agent with different concentrations.
- 4-The phantom will be imaged under full scatter conditions in conventional x-ray.
- 6- Evaluation of x-ray images.
- 7-Create a full model using CST MICROWAVE STUDIO® (CST STUDIO) program to calculate the electric field distribution.
- 8-Analysis the results

A colloidal Gold nanoparticle has been prepared by chemical reduction method as reported by Turkevich [6]. A solution of HAuCl₄ has been used as Au ions precursor, while sodium citrate has been used as both of mild reducing and stabilizing agent. The color of the solution slowly turned into faint pink color, indicating the reduction of the Au³⁺ ions to Au nanoparticles (Fig.4.a).

Optical Properties of colloidal Gold nanoparticle performed by UV-Vis absorption spectra were obtained on an Ocean Optics USB2000+VIS-NIR Fiber optics spectrophotometer.

Size and Shape of colloidal Gold nanoparticle determine by TEM performed on JEOL JEM-2100 high resolution transmission electron microscope at an accelerating voltage of 200 kV, respectively (Fig.5), (table.1) show the properties of colloidal Gold nanoparticle.

Table 1. Properties of colloidal Gold nanoparticle

| NPs | Gold |
|--------------------|-----------------|
| Appearance (Color) | Gradate Pink |
| Appearance (Form) | Liquid |
| Solubility | Water Soluble |
| Avg. Size | 5 nm diameter |
| Shape | Spherical shape |

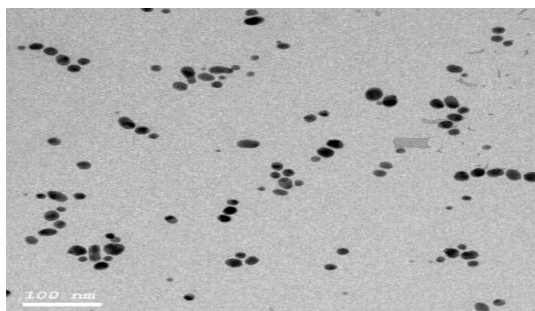


Figure 5. TEM micrograph of Gold nanoparticle

5. Experimental Analysis and Results

Using a fluoroscopic x-ray machine (Philips Duo-diagnost code RDXR001) 46 Kv and 5 mAs, was used to image the synthesized phantom before and after the injection of iodinated contrast agent and the nanoparticles into it.

The Hounsfield unit (HU) scale used in measurement is a linear transformation of the original linear attenuation coefficient measurement in one in which the radio density of distilled water at standard pressure and temperature (STP) is defined as zero Hounsfield units (HU), while the radio density of air at STP is defined as -1000 HU.

Thus, a change of one Hounsfield unit (HU) represents a change of 0.1% of the attenuation coefficient of water since the attenuation coefficient of air is nearly zero.

Figure .6 shows Hounsfield measurement for the five samples of nanoparticles with different concentration, which is demonstrated in table .2.

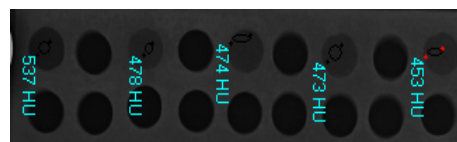


Figure 6. Measurement of HU of GNPs nanoparticles with different concentrations (0.1ml-0.05ml-0.025ml-0.0125ml-0.00625ml) using 46 KV and 5 mAs in x-ray image anterior posterior (AP) view.

In summary for the experimental results, by using fluoroscopic x-ray machine for scanning the phantom with different concentration of gold nanoparticles samples vary from 0.01 ml to 0.00625 ml), and performing Hounsfield measurements on the samples. Since HU measure the attenuation coefficient, It note that the HU measurement as shown in (table.2) start with a value of 537 at GNPs concentration of 0.1 ml and start to decrease gradually until it reach a value of 453 at GNPs concentration of 0.00625 with an attenuation percentage from the 1st sample of -8.4%.

Table 2. Change of Hounsfield for different concentration of Gold nanoparticle and its attenuation percentage

| Concentration(ml) | HU of GNPs | Attenuation % |
|-------------------|------------|---------------|
| 0.10000 | 537 | |
| 0.05000 | 478 | -5.9% |
| 0.02500 | 474 | -6.3% |
| 0.01250 | 473 | -6.4% |
| 0.00625 | 453 | -8.4% |

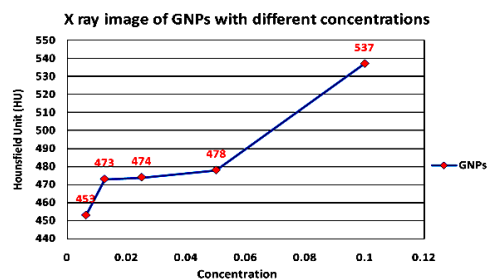


Figure 7. Measured HU with different concentration of GNPs in (AP) x-ray images using 46 Kv and 5 mAs.

Figure .7 shows a 2D representation of the results obtained from Fig .6 and table.2.

In conclusion for the experimental results, the reason for decreasing the HU measurement (attenuation decreasing) by decreasing the concentration is that when the concentration decrease the distance between GNPs increase and the electromagnetic coupling (electric field) between them decrease, to prove that a computational analysis and finite element simulation will be performed using CST STUDIO program.

6. Computational Simulations and Results

6.1. Determination of Gap Distance between GNPs

Because of nanoparticles tiny size, atoms and molecules cannot be counted by direct observation. But much as we do when "counting" beans in a jar, we can estimate the number of particles in a sample of an element or compound if we have some idea of the volume occupied by each particle and the volume of the container.

By knowing the following:

- 1- The concentration of the sample,
- 2- The volume of single GNPs.

We can determine the gap distance between two neighboring GNPs ,since the radius of a single GNPs which is (2.5 nm) , so the volume of it can be determined , by multiply volume of a single GNPs by the density of each sample we get the mass of a single GNPs , by dividing the total mass by the mass of a single GNPs we get the total number of GNPs in each concentration in cm³

We can do the following to calculate the gap distance between GNPs for different concentration:

- 1- After calculating the total number of GNPs in each concentration in cm³ ,
- 2- Taking the cubic root we get the number of GNPs in a one cm³,
- 3-Taking the inverse of the number of GNPs in a one cm we get the space between GNPs in cm units,
- 4-Multiplying this space by 107, we get the space between GNPs in nm units.

By applying the previous four steps for the GNPs of the five concentrations (0.1ml, 0.05ml, 0.025ml, 0.0125ml and 0.00625ml) a gap distance (S) between GNPs (Figure.8) calculated as shown in (Table 3), and fig 9.a.

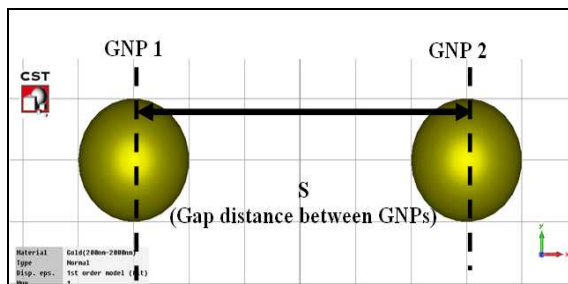
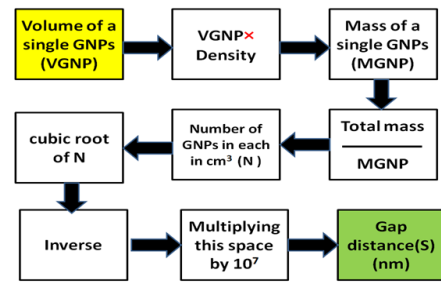


Figure 8. Gap distance (S) between GNPs.

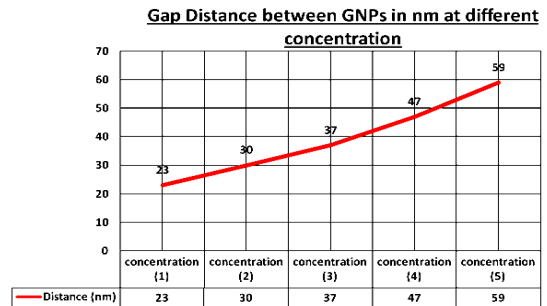
Table 3. Gap distance (S) between GNPs for different concentration

| Concentration(ml) | | Gap distance(S) between GNPs (nm) |
|-------------------|---------|-----------------------------------|
| Concentration(1) | 0.10000 | 23 |
| Concentration(2) | 0.05000 | 30 |
| Concentration(3) | 0.02500 | 37 |
| Concentration(4) | 0.01250 | 47 |
| Concentration(5) | 0.00625 | 59 |

Figure .9 shows the gap distance (S) change for different concentration, it note that by decreasing the concentration the gap distance increases, i.e we have indirect proportion between GNPs concentration and gap distance (S).



(a)



(b)

Figure 9. (a) Calculation diagram for gap distance calculation , (b)Gap distance (S) between GNPs for different concentration

6.2. The Model

The modeling and simulation was performed in CST STUDIO SUITE electromagnetic simulation software. Preliminary simulation and proof of concept were conducted in CST STUDIO Designer, while the complete simulation was conducted in CST STUDIO frequency domain solve.

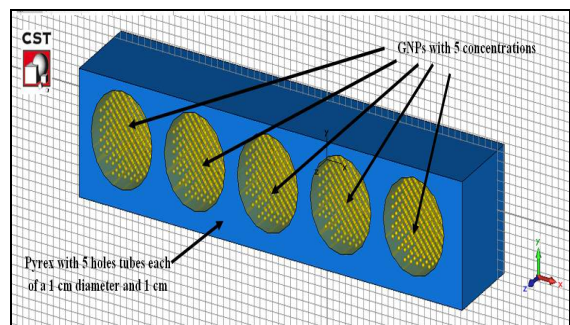


Figure 10. The Phantom model simulated in CST STUDIO.

Figure 10. shows the phantom model represented in CST STUDIO, which consists of five Pyrex tubes of a 1 cm diameter and 1 cm height filled with GNPs with 5 concentrations.

6.3. Simplify the Calculation

By making a simple mathematical calculation for the tube volume which is a cylinder, and a single GNPs with Spherical shape, we get the total count of GNPs in concentration(1) which is equal approximately 12×10^6 GNPs.

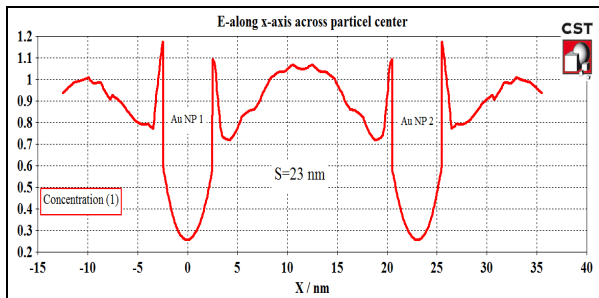
In order to keep the problem under a simple limits of complexity, the simulation will be performed on a two neighbor GNPs.

6.4. Electric Field Simulation for the Five Concentrations

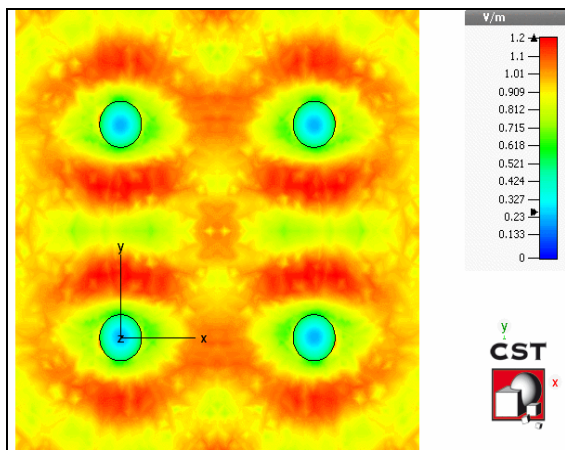
Simulation performed in six steps:

1- Step from 1 to 5, is the simulation of electric field (EF) intensity at both the gap distance (S) between GNPs and at the edges of GNPs for the five concentrations according to the change of gap distances (s) (23, 30, 37, 47 and 59 nm).

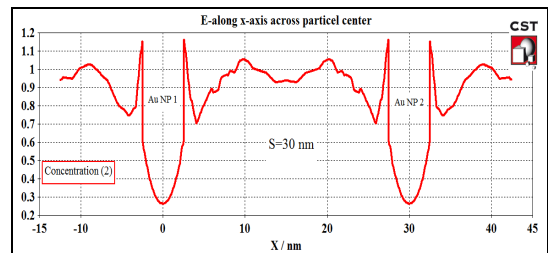
2- Merge the results obtained from step 1 to 5 to study the relation between gap distance change due concentration change and the EF intensity values which effect on the X-ray diagnoses.



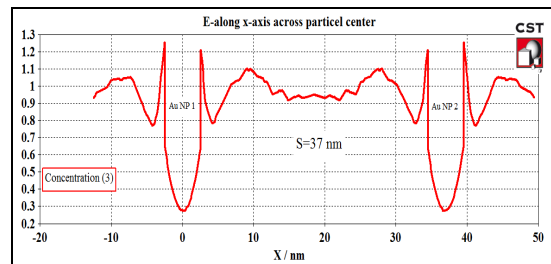
(a)



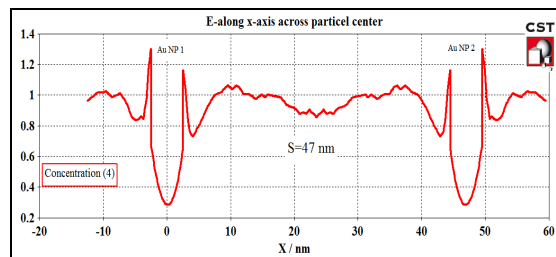
(b)



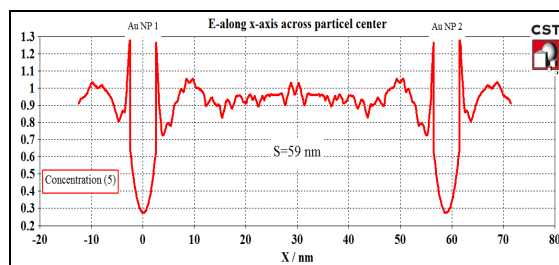
(a)



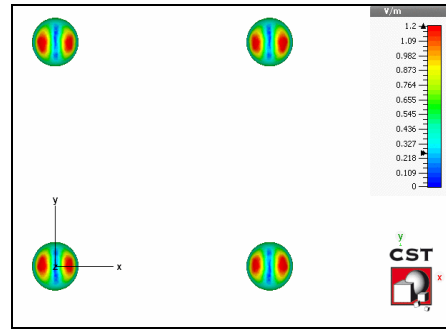
(b)



(c)



(d)



(c)

Figure 11. The Electric field (EF) intensity distribution for GNPs for concentration (1), (a) 2D of EF intensity, (b) EF intensity distribution, (c) 3D EF intensity

Figure 12. The 2D Electric field (EF) intensity, (a) concentration (2), (b) concentration (3), (c) concentration (4), (d) concentration (5)

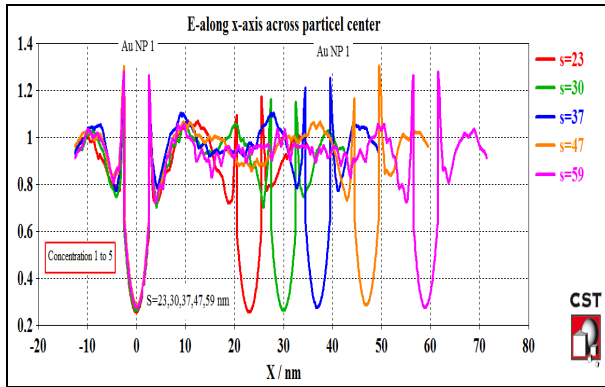


Figure 13. The 2D Electric field (EF) intensity after merging the results of the five concentrations

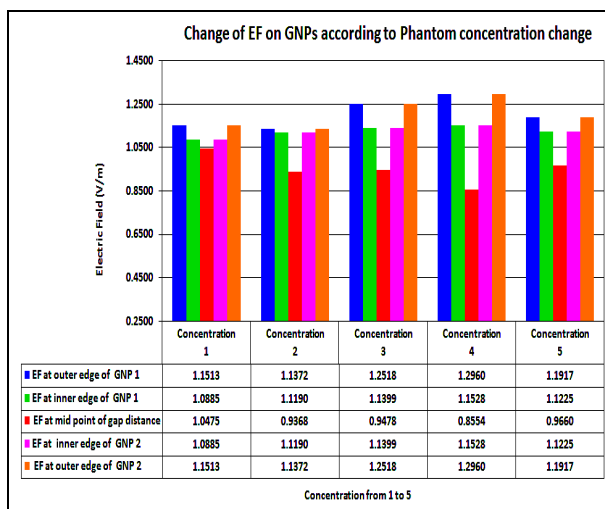


Figure 14. The 2D Electric field (EF) intensity at midpoint of gap distance (red), outer edges of GNPs 1 (blue), inner edges of GNPs 1 (green), outer edges of GNPs 2 (orange), and inner edges of GNPs 2 (pink),

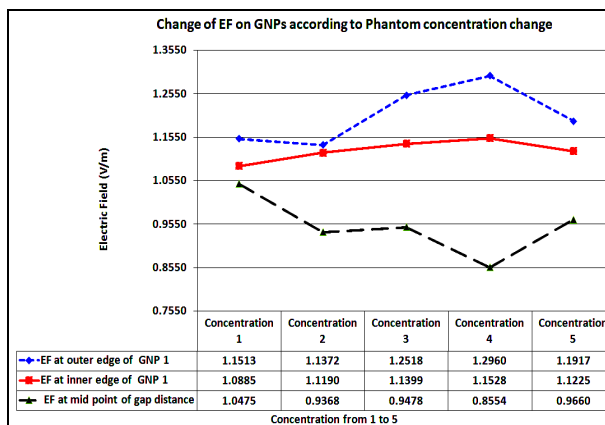


Figure 15. The 2D Electric field (EF) intensity on midpoint of gap distance and outer, inner edges of GNP

From figures (11 to 15) and table.4 which represent the EF intensity distribution on the gap distance between GNPs and on the inner and outer edges of them for the five concentrations of GNPs, the following results noted:

1-By decreasing the concentrations the gap distances (S)

increases gradually from (23 nm) at concentration (1), until it reach (59 nm) at concentration (5),

2- The multipacks electric field at the gap distance decreases gradually from (1.0475V/m) at concentration (1), until it reach (0.9660 V/m) at concentration (5).

3-The EF at the inner edges of GNPs fluctuated during the five concentrations between (1.0885 V/m) and (1.1528V/m).

3-The EF at the inner edges of GNPs fluctuated during the five concentrations between (1.2960 V/m) and (1.1372V/m).

4-The average of EF intensity of all EF value (midpoint, outer edges of GNPs 1, inner edges of GNPs 1, outer edges of GNPs 2, and inner edges of GNPs 2) have value ≈ 1 V/m.

Table 4. The value of EF intensity (V/m) at midpoint of gap distance, outer edges of GNPs 1, inner edges of GNPs 1, outer edges of GNPs 2, and inner edges of GNPs 2

| Concentration | Electric Field (V/m) at | | | | |
|---------------|-------------------------|---------------------|--------------------------|---------------------|---------------------|
| | outer edge of GNP 1 | inner edge of GNP 1 | midpoint of gap distance | inner edge of GNP 2 | outer edge of GNP 2 |
| 1 | 1.1513 | 1.0885 | 1.0475 | 1.0885 | 1.1513 |
| 2 | 1.1372 | 1.1190 | 0.9368 | 1.1190 | 1.1372 |
| 3 | 1.2518 | 1.1399 | 0.9478 | 1.1399 | 1.2518 |
| 4 | 1.2960 | 1.1528 | 0.8554 | 1.1528 | 1.2960 |
| 5 | 1.1917 | 1.1225 | 0.9660 | 1.1225 | 1.1917 |

7. Conclusion

In conclusion, electric field measurements were presented of metal gold nanoparticle at five different concentrations prove that the contrast agent GNPs can be used for the noninvasive, in vivo detection of X-ray diagnoses with high resolution and specificity, since the electric field intensity has a greater value on gap distance between GNPs and on its edges w.r.t the electric field intensity on other areas, the result show that the electric field intensity at the midpoint between neighboring GNPs decreases gradually due to the decreases of the gap distances between them due to the decreases of the concentration, Although the EF intensity at the midpoint decreases by the decreasing of the concentration, the EF intensity average of (midpoint, outer edges of GNPs 1, inner edges of GNPs 1, outer edges of GNPs 2, and inner edges of GNPs 2) fluctuated but have approximately constant value ≈ 1 V/m.

Acknowledgements

Authors wish to thank the editorial board and reviewers of cancer research journal. First author, Dr. Mohamed I. Badawi wishes to acknowledge to Prof .Dr. Moustafa M. Ahmed for his voluble help and support.

References

- [1] Jadzinsky, P.D.; Calero, G.; Ackerson, C.J.; Bushnell, D.A.; Kornberg, R.D. Structure of a thiol monolayer-protected gold nanoparticle at 1.1 Å resolution. *Science* 2007, 318, 430–433.

- [2] Röntgen, W.C. On a new kind of rays. *Nature* 1896, 53,
- [3] Paciotti GF, Myer L, Weinreich D, Goia D, Pavel N, McLaughlin RE, Tamarkin L. 2004. Colloidal gold: a novel nanoparticle vector for tumor directed drug delivery. *Drug Deliv* 11:169–183.
- [4] Faraday M. 1857. Experimental relations of gold (and other metals) to light. *Phil Trans R Soc London* 14:145–181.
- [5] Laaksonen, K., Suomela, S., Puisto, S.R., Rostedt, N.K.J., Ala-Nissila, T., and Nieminen, R.M., Influence of high-refractive-index oxide coating on optical properties of metal nanoparticles, *JOSAB*, Vol. 30, Issue 2, pp. 338-348 (2013)
- [6] 14. Turkevich, J.; Stevenson, P. C.; Hiller, J. *Discuss. Faraday Soc.* 1951, 11,
- [7] M I . Badawi , Moustafa M. Ahmed "Gold nanoparticles as high-resolution imaging contrast agent for early cancer diagnoses: Computational study" The 14th Arab International Conference of Materials Science "Materials for Biomedical Applications December 2013.
- [8] M I . Badawi , Moustafa M. Ahmed "Gold nanoparticles as high-resolution imaging contrast agent for early cancer diagnoses: Computational study" *International Journal of Chemical & Applied Biological Sciences*, April 2014. 274–276.